01 Jul 1999

A Blind Deconvolution Approach for Resolution Enhancement of Near-Field Microwave Images

Ali Mohammad-Djafari

Nasser N. Qaddoumi

R. Zoughi
Missouri University of Science and Technology, zoughi@mst.edu

Recommended Citation

A. Mohammad-Djafari et al., "A Blind Deconvolution Approach for Resolution Enhancement of Near-Field Microwave Images," *Proceedings of Mathematical Modeling, Bayesian Estimation, and Inverse Problems (1999: Denver, CO)*, vol. 3816, pp. 274-281, SPIE--The International Society for Optical Engineering, Jul 1999.
The definitive version is available at https://doi.org/10.1117/12.351322

A BLIND DECONVOLUTION APPROACH FOR RESOLUTION ENHANCEMENT OF NEAR-FIELD MICROWAVE IMAGES

Ali Mohammad–Djafari[1], Nasser Qaddoumi[2] and Reza Zoughi[2]

[1] Laboratoire des Signaux et Systèmes (CNRS–SUPELEC–UPS)
École Supérieure d'Électricité
Plateau de Moulon, 91192 Gif–sur–Yvette Cedex, France
E-mail: djafari@lss.supelec.fr

[2]Applied Microwave NDT Lab.
Electrical and Computer Engineering Dept., Colorado State University
Fort Collins, CO 80523-1373
E-mails: qaddoumi@engr.colostate.edu zoughi@engr.colostate.edu

ABSTRACT

In this paper we propose a blind deconvolution method to enhance the resolution of images obtained by near-field microwave nondestructive techniques using an open ended rectangular waveguide probe. In fact, we model such images to be the result of a convolution of the real input images with a point spread function (PSF). This PSF depends mainly on the dimensions of the waveguide, the operating frequency, the nature of the object under test and standoff distance between the waveguide and the object. Unfortunately, it is very difficult to model this PSF from the physical data. For this reason, we consider the problem as a blind deconvolution. The proposed method is based on regularization, and the solution is obtained iteratively, by successive estimations of the input and the PSF. The algorithm is initialized with a PSF obtained from a very simplified physical model. The performance of the proposed method is evaluated on some real data. Several examples of real image enhancement will be presented.

Keywords: Microwave Nondestructive Testing, Near-field Imaging, Blind Image restoration

1. INTRODUCTION

In recent years, near-field microwave nondestructive testing techniques have shown great promise in many applications including image production of interior defects in a variety of composite structures. When operating in the near-field of a probe, the spatial resolution associated with such images is primarily a function of the probe dimensions. To increase the resolution of such images obtained using a rectangular waveguide probe, we model an image to be the result of a convolution of the real input image and a point spread function (PSF). This PSF depends mainly on the dimensions of the waveguide, the operating frequency, the nature of the object under test and standoff distance between the waveguide and the object. Unlike the plane-wave far-field approach, the PSF associated with these probes strongly depends on the distance away from the probe, and it is not simple to model this PSF from the physical data. For this reason, we consider the problem as a blind deconvolution.

The proposed method is based on regularization, and the solution is defined as the optimum of a criterion which has three parts: a data fitting part and two regularization functions on the input and on the impulse response. The solution is obtained iteratively, by successive estimations of the input and the PSF. We first consider a quadratic criterion for these three parts. This results in linear operations for both steps of PSF and input estimations. Unfortunately, this approach does not seem to give satisfactory results. This is due to the fact that, the resulting criterion is not a convex function of both PSF and the input even if it is quadratic in each of them separately. We then consider the case where we may have more than two sets of data on the same object (multi-channel blind deconvolution approach). Again, we first consider a quadratic criterion which results to linear operations on the

Reza Zoughi was on sabbatical with Supélec during the fall 1998 semester. Appeared in Proceedings of SPIE99, Denver, CO, USA, Vol. 3816, pp: 274-281, July 1999.

data for point spread functions of each channel and input estimation. But, here again, this approach does not give satisfactory results.

As a consequence of these conclusions, we propose a method which seems to be adequate for the special cases in which we are looking at binary or two levels images (homogeneous background surronding a homogeneous fault region). This is, in fact, the actual situation in many non destructive testing applications. The proposed algorithm is an iterative one in which, at each iteration, a linear filtering of the data followed by a nonlinear memoriless operation gives an estimate of the input which is then used to obtain an estimate of the PSF by another linear filtering operation. The non-linear operation is an evolutif sigmoid-like function whose hardness is increased during the iterations.

This paper is organized as follows: In section 2 we present the linear blind deconvolution, first the case of single channel and then the multi-channel one. In section 3 we present our non-linear algorithm for both cases. In section 4 we present some numerical results to show the performances of the proposed algorithms on simulated data, and finally, in section 5 we present the results of the proposed algorithms on a few real data.

2. BLIND DECONVOLUTION

To introduce the proposed method, we first present a synthetique view of the linear techniques of blind deconvolution which have been developped and used by many authors.[1–6] We consider first the case where we have only one set of data (single channel blind deconvolution) and then the case where we may have two or more sets of data for a given object (multi-channel blind deconvolution). Then, we analyze the limits of linear techniques and, finally, we propose our nonlinear technique for both single and multi-channel case.

2.1. Single-channel linear blind deconvolution

In linear deconvolution techniques, the relation between the input and the output images is modelled by a 2D convolution equation :

$$g(x,y) = h(x,y) * f(x,y) + n(x,y) \tag{1}$$

where $h(x,y)$ is the PSF of the measurement system, and $n(x,y)$ models all the errors including modeling and measurement noise. $n(x,y)$ is generally assumed to be a centered, white and Gaussian random function. The solution of the problem is defined to be the optimum of the following regularization criterion :

$$J(f,h) = \|g - h * f\|^2 + \lambda_f \|d_f * (f - f_0)\|^2 + \lambda_h \|d_h * (h - h_0)\|^2 \tag{2}$$

where $d_f(x,y)$ and $d_h(x,y)$ are the PSFs of two derivating functions, λ_f and λ_h are two regularization parameters, $f_0(x,y)$ and $h_0(x,y)$ are the *a priori* solutions for $f(x,y)$ and $h(x,y)$ and $\|f\|^2 = \iint |f(x,y)|^2 \, \mathrm{d}x \, \mathrm{d}y$. Derivating this criterion with respect to its unknowns separetely, we obtain :

$$\left\{ \begin{array}{rcl} \frac{\partial J}{\partial f} & = & -2\,\bar{h} * [g - h * f] + 2\,\lambda_f\,\bar{d}_f * [d_f * (f - f_0)] \\ \frac{\partial J}{\partial h} & = & -2\,\bar{f} * [g - h * f] + 2\,\lambda_h\,\bar{d}_h * [d_h * (h - h_0)] \end{array} \right. \tag{3}$$

where $\bar{h}(x,y) = h(-x,-y)$, $\bar{f}(x,y) = f(-x,-y)$, $\bar{d}_f(x,y) = d_f(-x,-y)$ and $\bar{d}_h(x,y) = d_h(-x,-y)$. Thus, the optimal solution satisfies the following equations:

$$\left\{ \begin{array}{l} \left[\bar{h} * h + \lambda_f\,\bar{d}_f * d_f\right] * f = \bar{h} * g + \lambda_f\,\bar{d}_f * [d_f * f_0] \\ \\ \left[\bar{f} * f + \lambda_h\,\bar{d}_h * d_h\right] * h = \bar{f} * g + \lambda_h\,\bar{d}_h * [d_h * h_0] \end{array} \right. \tag{4}$$

which, in the Fourier domain, become:

$$\left\{ \begin{array}{rcl} \left[|H(u,v)|^2 + \lambda_f\,|D_f(u,v)|^2\right]\,F(u,v) & = & H^*(u,v)\,G(u,v) + \lambda_f\,|D_f(u,v)|^2\,F_0(u,v) \\ \left[|F(u,v)|^2 + \lambda_h\,|D_h(u,v)|^2\right]\,H(u,v) & = & F^*(u,v)\,G(u,v) + \lambda_h\,|D_h(u,v)|^2 H_0(u,v) \end{array} \right. \tag{5}$$

and so we obtain:

$$F(u,v) = \frac{H^*(u,v)\,G(u,v) + \lambda_f\,|D_f(u,v)|^2\,F_0(u,v)}{|H(u,v)|^2 + \lambda_f\,|D_f(u,v)|^2} \tag{6}$$

$$H(u,v) = \frac{F^*(u,v)\,G(u,v) + \lambda_h\,|D_h(u,v)|^2 H_0(u,v)}{|F(u,v)|^2 + \lambda_h\,|D_h(u,v)|^2} \tag{7}$$

These two last equations are very familiar for the case where $f_0(x,y) = 0$ and $h_0(x,y) = 0$.

When the parameters λ_f and λ_h and the functions $d_f(x,y)$, $d_h(x,y)$, $f_0(x,y)$ and $h_0(x,y)$ are fixed, one can obtain a solution corresponding to a local optimum of (2) by an iterative algorithm such as :

0. Initialize $h(x,y)$ to $h_0(x,y)$ and repeat until convergence:
1. Compute $F(u,v)$ from (6) and then $f(x,y)$ by IDFT ;
2. Compute $H(u,v)$ from (7) and then $h(x,y)$ by IDFT ;

or

0. Initialize $f(x,y)$ to $f_0(x,y)$ and repeat until convergence:
1. Compute $H(u,v)$ from (7) and then $h(x,y)$ by IDFT ;
2. Compute $F(u,v)$ from (6) and then $f(x,y)$ by IDFT .

But, unfortunately, in practical applications, two difficulties arise:

- Even when λ_f, λ_h, $d_f(x,y)$, $d_h(x,y)$, $f_0(x,y)$ and $h_0(x,y)$ are fixed and even if the criterion (2) is quadratic in both f and h separately, it is not a convex function of both of them and it can have many local optima. Thus, to obtain a unique satisfactory solution, we need a stronger constraint on the solution. One way to do this is to constrain the input f to be a piecewise constant function. Indead, in our application, this constraint is in fact a wish: for example, when we are searching for a default region in a safe homogeneous region, we are looking for an image $f(x,y)$ which is a binary valued. In the next section we will see how we can impose these kind of constraints to obtain satisfactory results.

- Another main issue in this algorithm is the initialization. As we mentionned, this algorithm converges to a local optimum of the criterion (2). Thus the initialization of the algorithm may have a great influence on the solution. We propose to use the physical knowledge of the measurement system to obtain an initial estimate for the impulse response. For example, if we assume that the standoff of the sensor waveguide is zero, then a good approximation for the impulse response is given by

$$h^0(x,y) = \begin{cases} \cos(\pi x/2a) & x \in [-a/2, a/2], y \in [-b/2, b/2] \\ 0 & elsewhere, \end{cases} \tag{8}$$

- Finally, in practical situations, we have to fix the parameters λ_f and λ_h, the functions $d_f(x,y)$, $d_h(x,y)$ and the *a priori* solutions $f_0(x,y)$ and $h_0(x,y)$. What we propose here is the following :
  $d_f(x,y)$ and $d_h(x,y)$ are respectively chosen as separable first and second order derivative operators;
  $f_0(x,y) = g(x,y)$ and $h_0(x,y) = h^0(x,y)$ as in (8); and
  the two regularization parameters are fixed experimentally to $\lambda_f = \frac{1}{H_0(0)}$ and $\lambda_h = \frac{1}{F_0(0)}$.

2.2. Multi-channel linear blind deconvolution

In some experiments, we may have more than one set of data, each obtained with a different sensor:

$$g_i(x,y) = h_i(x,y) * f(x,y) + n_i(x,y), \quad i = 1, \cdots, M \tag{9}$$

where the problem here is to estimate simultaneously $f(x,y)$ and all the PSF's $h_i(x,y), i = 1, \cdots, M$. We again can define the solution as the optimizer of the following criterion

$$J(f, h_f, \cdots, h_M) = \sum_{i=1}^{M} \|g_i - h_i * f\|^2 + \lambda_f \|d_f * (f - f_0)\|^2 + \lambda_h \sum_{i=1}^{M} \|d_h * (h_i - h_{i_0})\|^2 \tag{10}$$

The solution has to satisfy

$$\left\{ \begin{array}{rcl} \dfrac{\partial J}{\partial f} & = & -2 \sum_{i=1}^{M} \bar{h}_i * [g_i - h_i * f] + 2\,\lambda_f\, \bar{d}_f * [d_f * (f - f_0)] \\ \dfrac{\partial J}{\partial h_i} & = & -2\,\bar{f} * [g_i - h_i * f] + 2\,\lambda_h\, \bar{d}_h * [d_h * (h_i - h_{i_0})], \quad i = 1, \cdots, M \end{array} \right. \tag{11}$$

which, in the Fourier domain, become

$$\left\{ \begin{array}{rcl} \left[\sum_{i=1}^{M} |H_i(u,v)|^2 + \lambda_f\, |D_f(u,v)|^2 \right] F(u,v) & = & \sum_{i=1}^{M} H_i^*(u,v)\, G_i(u,v) + \lambda_f\, |D_f(u,v)|^2 F_0(u,v) \\ \left[|F(u,v)|^2 + \lambda_h\, |D_h(u,v)|^2 \right] H_i(u,v) & = & F^*(u,v)\, G_i(u,v) + \lambda_h\, |D_h(u,v)|^2 H_{i_0}(u,v), \quad i = 1, \cdots, M \end{array} \right. \tag{12}$$

and so we obtain:

$$F(u,v) = \frac{\sum_{i=1}^{M} H_i^*(u,v)\, G_i(u,v) + \lambda_f\, |D_f(u,v)|^2\, F_0(u,v)}{\sum_{i=1}^{M} |H_i(u,v)|^2 + \lambda_f\, |D_f(u,v)|^2} \tag{13}$$

$$H_i(u,v) = \frac{F^*(u,v)\, G_i(u,v) + \lambda_h\, |D_h(u,v)|^2\, H_{i_0}(u,v)}{|F(u,v)|^2 + \lambda_h\, |D_h(u,v)|^2}, \quad i = 1, \cdots, M \tag{14}$$

We can again propose the following algorithm to obtain the solution:
0. Initialize $h_i(x,y)$ to $h^0(x,y)$ and repeat until convergence:
1. Compute $F(u,v)$ from (13) and then $f(x,y)$ by IDFT ;
2. Compute $H_i(u,v)$ from (14) and then $h_i(x,y)$ by IDFT ;

We can also imagine to select one set of the data (say g_f) and do the following:
0. Initialize $h_1(x,y)$ to $h_{1_0}(x,y)$ and first compute $F(u,v)$ from (6) and then repeat until convergence:
1. Compute $F(u,v)$ from (13) and then $f(x,y)$ by IDFT ;
2. Compute $H_i(u,v)$ from (14) and then $h_i(x,y)$ by IDFT ;

3. PROPOSED METHOD

Blind image restoration is an ill posed problem. It is easy to show that any linear method can not give satisfactory results. Hence, we propose a non-linear method. The specificity of our approach is on the way we model the image generation: we model the input image as the output of an autoregressive (AR) process followed by a memoriless nonlinear operation $q(.)$ as is illustrated in the following:

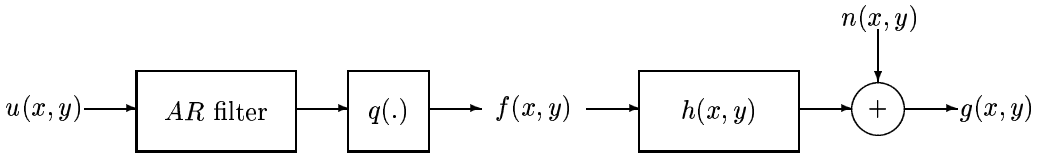

Figure 1. Proposed data generation model.

Then, again as in (2), we can define the solution of the problem as the optimum of the following regularization criterion :

$$J(f,h) = \|g - h * f\|^2 + \lambda_f\, \|q\,(d_f * (f - f_0))\,\|^2 + \lambda_h\, \|d_h * (h - h_0)\|^2 \tag{15}$$

and use a gradient based algorithm to obtain the solution. Noting that

$$\frac{\partial J}{\partial f} = -2\,\bar{h} * [g - h * f] + 2\,\lambda_f\,\bar{d}_f * r\,(d_f * (f - f_0)) \tag{16}$$

$$\frac{\partial J}{\partial h} = -2\,\bar{f} * [g - h * f] + 2\,\lambda_h\,\bar{d}_h * [d_h * (h - h_0)], \tag{17}$$

where $r(.) = q(.)\,q'(.)$, and that the second equation has an explicite solution given by (16), one possible algorithm is the following:

0. Initialize $h(x,y)$ to $h^0(x,y)$ and $f(x,y)$ to $f^0(x,y)$; and repeat until convergence:
1. Compute $\frac{\partial J}{\partial f}$ using (16);
2. Update f using $f^{(k+1)} = f^{(k)} + \alpha^{(k)} \frac{\partial J}{\partial f}\left(f^{(k)}, h^{(k)}\right)$
3. Update h using (7).

However, to obtain a fast algorithm for practical applications, we preferred to use the following scheme:

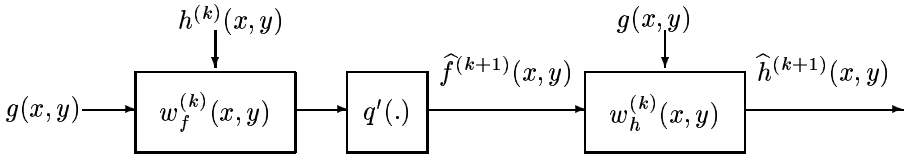

Figure 2. One iteration of the proposed blind restoration algorithm.

This algorithm is very interesting, because at each iteration, a linear transformation (chracterized by $w_f(x,y)$) followed by a memoriless non-linear action $g'(.)$ gives an update of f, and another linear transformation (chracterized by $w_h(x,y)$) gives an update of h:

The exact type of the non-linear function $q(.)$ is not really very important. The only needed property is a saturation like function at both sides such as a sigmoide function or a saturated linear function:

$$f(x,y) = \begin{cases} \bar{f}(\bar{\eta}) & \text{if} \quad f(x,y) > \bar{\eta} = f_{\min} + \alpha(f_{\max} - f_{\min}) \\ \frac{\bar{f} - \underline{f}}{\bar{\eta} - \underline{\eta}}(f(x,y) - \bar{\eta}) & \text{if} \quad \underline{\eta} < f(x,y) < \bar{\eta} \\ \underline{f}(\underline{\eta}) & \text{if} \quad f(x,y) < \underline{\eta} = f_{\min} + (1-\alpha)(f_{\max} - f_{\min}) \end{cases} \tag{18}$$

where $f_{\min}$ and $f_{\max}$ are the minimum and maximum values of $f(x,y)$ and α is either a constant ($\alpha = .5$) or a decreasing variable during the iterations (α has to start by 1 and to finish by 0.5 if we want to obtain a binary valued solution).

The same scheme can be applied to the multi-channel case. Its exapansion is omitted here, but we have implented it for the numerical simulations and real data processing.

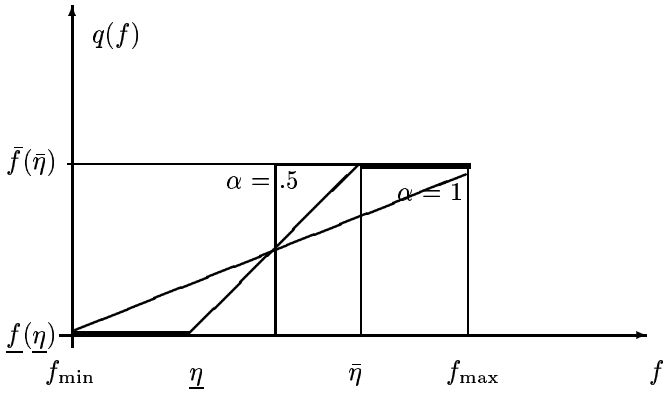

Figure 3. Memoriless non-linear operation. During the iterations $\bar{\eta}$ and $\underline{\eta}$ change: at the first iteration $\bar{\eta} = f_{\min}$ and $\underline{\eta} = f_{\max}$ and at the last iteration $\bar{\eta} = \underline{\eta} = \frac{1}{2}(f_{\max} - f_{\min})$.

4. SIMULATION RESULTS

The main objective of these numerical experimentations is to show that the proposed algorithm works well. The two following figures show two typical results for the case of single channel and two channels blind reconstruction.

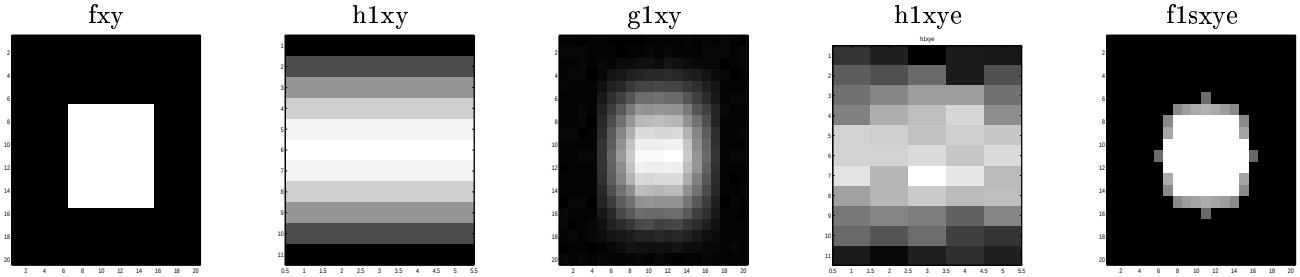

Figure 4. Single channel blind reconstruction:
a) original image, b) PSF, c) degraded image, d) PSF estimate, e) reconstruction

5. APPLICATION ON REAL DATA

The method outlined above was then applied on real data, in the form of 2-dimensional near-field microwave images. Near-field microwave imaging is based on transmitting a wave into a structure, which is located in the near-field of a sensor, and using a signal proportional to the magnitude and/or phase of the transmitted or reflected wave to create a two dimensional intensity image of the structure under investigation. The features and properties of microwave near-field images are influenced by several factors such as the dielectric and physical properties of the structure under investigation, the frequency of operation, the standoff distance and the dimensions of the waveguide. Also, the non-uniformity associated with the electric field distribution at the waveguide aperture influences the resulting near-field image. Due to all of these factors it is not possible to come up with a PSF that can be used to reconstruct the real input image and that is when the outlined blind deconvolution method becomes handy to obtain the real input image.

Near-field images of a patch of rust under paint on a steel specimen were used to demonstrate the capabilities of the blind deconvolution method. The specimen was produced by acquiring a relatively flat piece of steel on which a thin layer of rust had already been produced (naturally). Then, a 40 mm by 40 mm area was masked out by a piece of tape and the remaining surface was sand blasted. The average thickness of the rust layer was measured (using a micrometer) to be approximately 0.08 mm. Subsequently, this specimen was painted with 0.60 mm of common

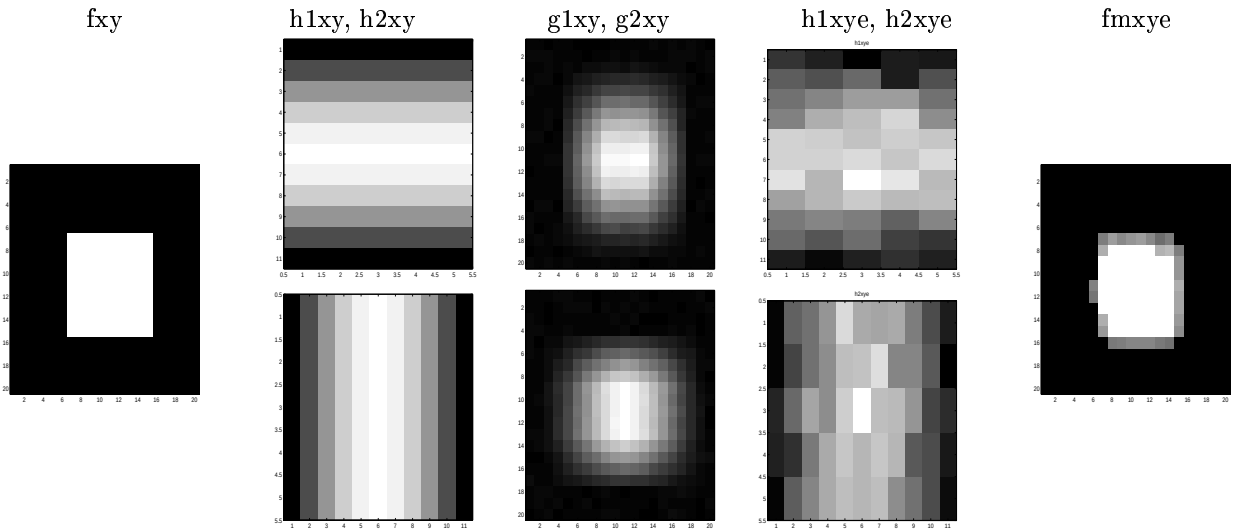

Figure 5. Two channels blind reconstruction:
a) original image, b) PSFs of the two channels, c) degraded images, d) PSFs estimates, e) reconstruction

spray paint, as uniformly as possible. 0.60 mm represents ten painting cycles. Consequently, microwave images of the rust specimen were produced using raster scans (every 2 mm by 2 mm) of the specimen at 33.5 GHz. For the raw data image shown, the measured voltage is normalized with respect to its maximum value and then different colors are assigned to different normalized voltages to produce an image. Therefore, from one image to another the color associated with the rusted area may differ.[7,8]

The following figures show some examples.

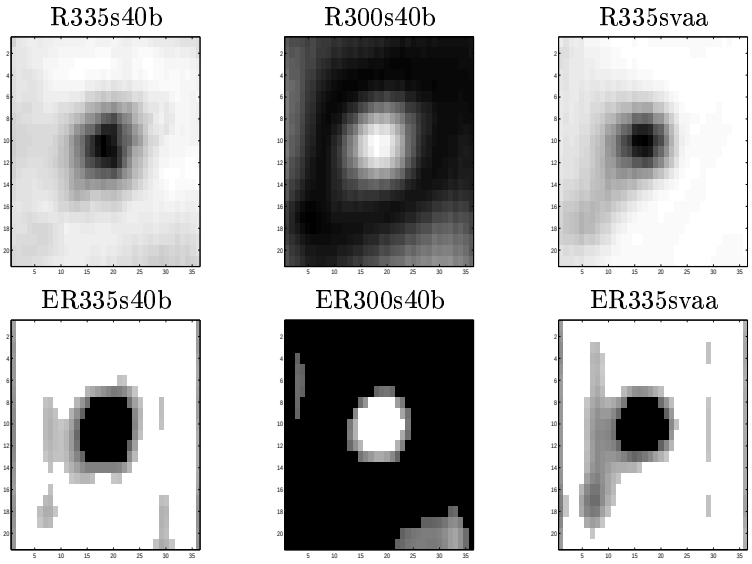

Figure 6. Single channel reconstructions: First raw the data, Second raw the reconstructions.

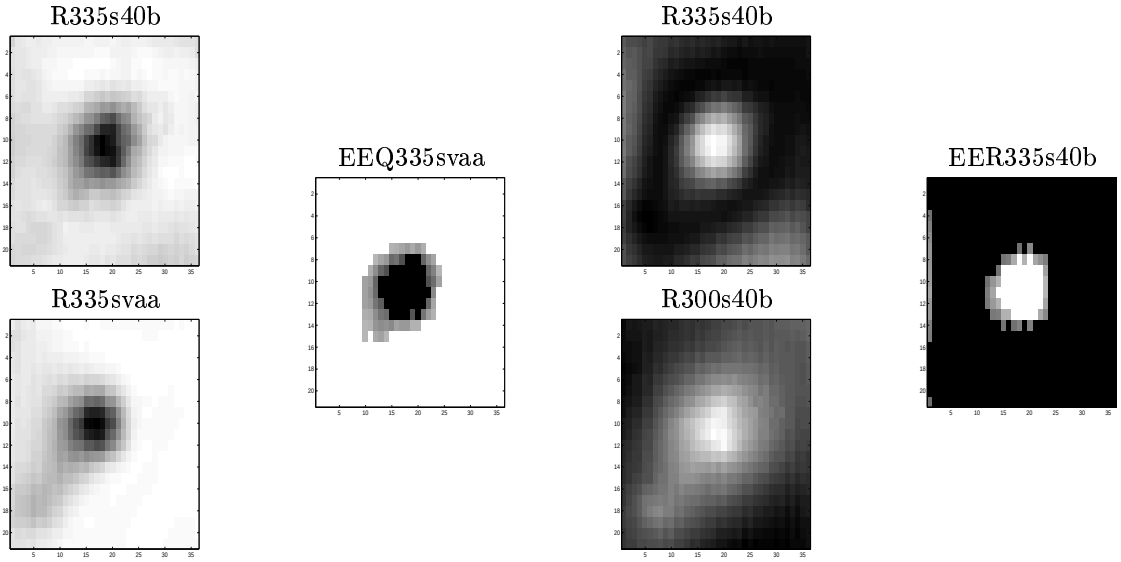

Figure 7. Multi channel reconstructions:
The image in column b is obtained using the two data sets in column a (`R335s40b and R335svaa`).
The image in column d is obtained using the two data sets in column c (`R335s40b and R300s40b`).

6. CONCLUSIONS

We proposed a non-linear blind deconvolution method to enhance the resolution of images obtained by near-field microwave nondestructive techniques. We first considered linear techniques, both single and muli-channel, but unfortunately, these techniques, even based on regularized criterion, did not give satisfactory results. Based on this conclusion, we proposed an iterative algorithm where at each iteration, a linear filtering followed by a memoriless non-linear transformation gives an update of the input, and another linear filtering gives an update of PSF. The algorithm is initialized with a PSF obtained from a very simplified physical model. The performances of the proposed method were evaluated on some real data.

REFERENCES

1. B. Hunt, "Bayesian methods in nonlinear digital image restoration," *IEEE Transactions on Communications* **C-26**, pp. 219–229, March 1977.
2. R. M. Leahy and C. E. Goutis, "An optimization technique for constraint based image restoration and reconstruction," *IEEE Transactions on Acoustics Speech and Signal Processing* **ASSP-34**, pp. 1629–1642, December 1986.
3. R. Lagendijk, J. Biemond, and D. E. Boekee, "Identification and restoration of noisy blurred images using the expectation minimization algorithm," *IEEE Transactions on Acoustics Speech and Signal Processing* **ASSP-38**, pp. 1180–1191, 1990.
4. S. Kuo and R. Mammone, "Image restoration by convex projections using adaptive constraints and the l_1 norm," *IEEE Transactions on Acoustics Speech and Signal Processing* **40**, pp. 159–168, January 1992.
5. J. K. Paik and A. K. Katsagellos, "Image restoration using a modified Hopfield network," *IEEE Transactions on Image Processing* **IP-1**, pp. 49–63, January 1992.
6. T. Schultz, "Multiframe blind deconvolution of astronomical images," *Journal of the Optical Society of America* **10**, May 1993.
7. N. Qaddoumi and R. Zoughi, "Preliminary Study of the Influences of Effective Dielectric Constant and Non-Uniform Probe Aperture Field Distribution on Near-Field Microwave Images," *Materials Evaluation*, vol. 55, no. 10, pp. 1169–1173, October, 1997.
8. N. Qaddoumi, A. Shroyer and R. Zoughi, "Microwave Detection of Rust Under Paint and Composite Laminates," *Research in Nondestructive Evaluation*, vol. 9, no. 4, pp. 201–212, 1997.